PNAS

Supporting Information for

Molecular mechanism underlying SNARE-mediated membrane fusion

enlightened by all-atom molecular dynamics simulations

Josep Rizo[a,b,c,1], Levent Sari[a,d], Klaudia Jaczynska[a,b,c], Christian Rosenmund[e,f], and Milo M. Lin[a,d]

[a]Department of Biophysics, University of Texas Southwestern Medical Center, Dallas, Texas 75390, USA

[b]Department of Biochemistry, University of Texas Southwestern Medical Center, Dallas, Texas 75390, USA

[c]Department of Pharmacology, University of Texas Southwestern Medical Center, Dallas, Texas 75390, USA

[d]Green Center for Systems Biology, University of Texas Southwestern Medical Center, Dallas, Texas 75390, USA

[e]Charité – Universitätsmedizin Berlin, corporate member of Freie Universität Berlin and Humboldt-Universität zu Berlin, Institute of Neurophysiology, Berlin, Germany

[f]NeuroCure Cluster of Excellence, Berlin, Germany.

[1]To whom correspondence may be addressed. Email: Jose.Rizo-Rey@UTSouthwestern.edu

This PDF file includes:

Other supporting materials for this manuscript include the following:

Movie S1

Supporting Discussion

Limitations of our MD simulations

The fact that all-atom MD simulations are computationally very intensive limits the length of time that can be simulated, particularly for systems of millions of atoms such as those studied here. Thus, we were able to perform only one simulation in the 1-2 μs time scale for each of the configurations presented. Ideally, multiple replicas should be computed with longer time scales, employing different force fields and different initial configurations to draw firm conclusions. Moreover, our results were obtained at 350 K to help overcome energy barriers within the time scales that we could simulate, which would require much longer simulation times at 310 K. Nevertheless, it is important to note that the fundamental physicochemical properties of the system are not expected to be substantially altered by the high temperature used, based on our knowledge on the physicochemical properties of proteins and lipids. Their behavior depends on a combination of non-bonding interactions, including hydrophobic, hydrogen bonding and electrostatic interactions. The relative importance of these interactions can change gradually with the temperature, but the main undesirable consequence of increasing the temperature for proteins is unfolding, which we did not observe. In fact, two syntaxin-1 molecules became fully helical during the simulation that led to membrane fusion (Fig. 5). We also did not observe any anomaly in the overall membrane structure and dynamics away from the fusion site. Note also that, for membranes, it is common to increase the temperature in MD simulations to increase lipid fluidity [e.g. refs. (1, 2), which used 350 K and 350-370 K, respectively]. Moreover, a systematic analysis of several physical properties of membranes with diverse lipid compositions by all-atom MD simulations using CHARMM36, the same force field that we employed, showed an excellent agreement between the values predicted with MD simulations at temperatures ranging from 293 to 333 K and the experimentally determined values (3).

SNAREs cannot be viewed as pre-formed helical rods

Extensive evidence shows that SNARE proteins undergo multiple structural changes during the steps that lead to synaptic vesicle tethering, priming and fusion, and do not act as pre-formed helical rods. Thus, SNARE motifs have a tendency to form helical structures, but they are unstructured in isolation (4-6). Assembly of the SNARE four-helix bundle is templated by Munc18-1 when it binds to synaptobrevin and syntaxin-1, bringing the N-termini of their SNARE motifs together while their C-termini are distant from each other (7, 8) and are flexibly linked to their respective TM regions (9). Moreover, continuous synaptobrevin and syntaxin-1 helices would be energetically unfavorable in a trans-configuration because of the geometrical constraints. Consistent with these predictions, our attempts to generate trans-SNARE complexes through restrained MD simulations led to loss of helical conformation at the linkers or formation of kinks at the linker helices [(10), Fig. S1*C,D*, S5*A*). Importantly, formation of a continuous helix is clearly not required for the function of synaptobrevin and, actually, flexibility in its TM region is important for release (11-14) (see Discussion).

Linker zippering is more critical for Ca^{2+}-triggered neurotransmitter release than for slower forms of release

While the 259GSG insertion before the syntaxin-1 jxt linker abolishes Ca^{2+}-triggered release and the 265GSG insertion after the jxt linker strongly reduces de amplitude but not the charge of Ca^{2+}-triggered release, these mutations had milder effects on other forms of release that occur at slower time scales. Thus, the 259GSG and 265GSG insertions in syntaxin-1 lead to 75% and 60% reductions, respectively, in release induced by hypertonic sucrose, which is used to measure the readily-releasable pool of synaptic vesicles (15). These results indicate that linker zippering also facilitates release on the slower time scales of these experiments but is not as crucial as it is for fast Ca^{2+}-evoked release, and that extension of the jxt

helix into the TM region also helps but is not essential for sucrose-induced release. Spontaneous neurotransmitter release was not substantially altered by the 259GSG insertion but was enhanced three-fold by the 265GSG insertion (15, 16), indicating that spontaneous release does not require linker zippering but somehow depends on coupling between the jxt linker and the TM region of syntaxin-1.

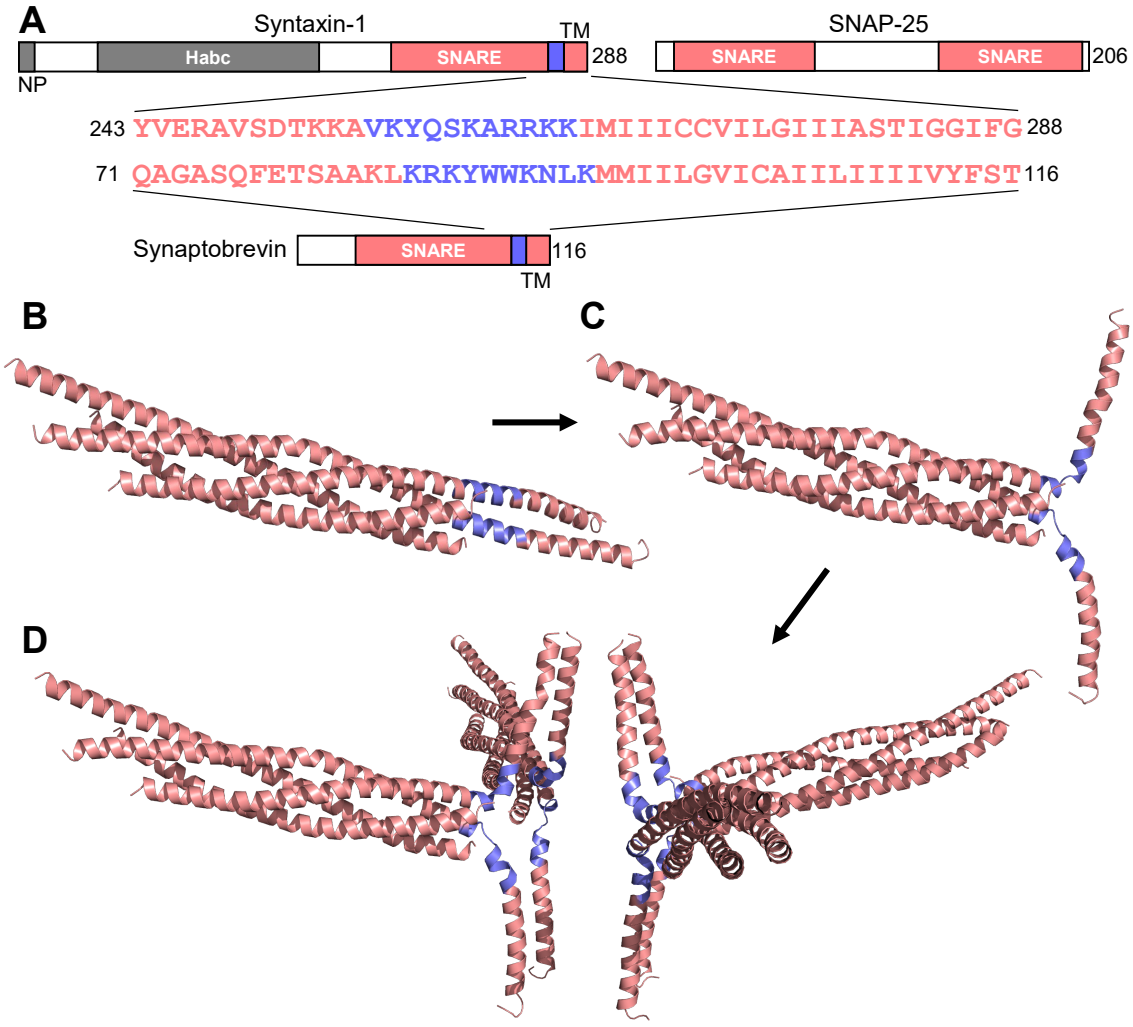

Figure S1. Generation of almost completely helical trans-SNARE complexes. (*A*) Domain sequences of syntaxin-1, SNAP-25 and synaptobrevin, with the SNARE motifs and TM regions in salmon, and the jxt linkers in blue. Numbers on the right of the diagrams show the length of each protein. NP = N-peptide; SNARE = SNARE motif; TM = transmembrane. The sequences of the C-terminal residues of the SNARE motifs, the jxt linkers and the TM regions of syntaxin-1 and synaptobrevin are shown. (*B*) Ribbon diagram of the crystal structure of the neuronal cis-SNARE complex (17) (PDB accession number 3HD7), which was used as starting point for restrained MD simulations used to generate trans-SNARE complexes. The N-terminal region of syntaxin-1 containing the N-peptide and the H_{abc} domain is not part of the structure and was not included in any of the MD simulations described here. (*C*) Ribbon diagram of the trans-SNARE complex generated by restrained MD simulations with mild force constants to minimally perturb the conformations of the jxt linkers. (*D*) Ribbon diagram of the four trans-SNARE complexes obtained by rotations and translations of the complex shown in (*C*), after they were incorporated in the fusion2g system and the temperature and pressure of the system were equilibrated. The jxt linkers are colored in blue in (*B-D*).

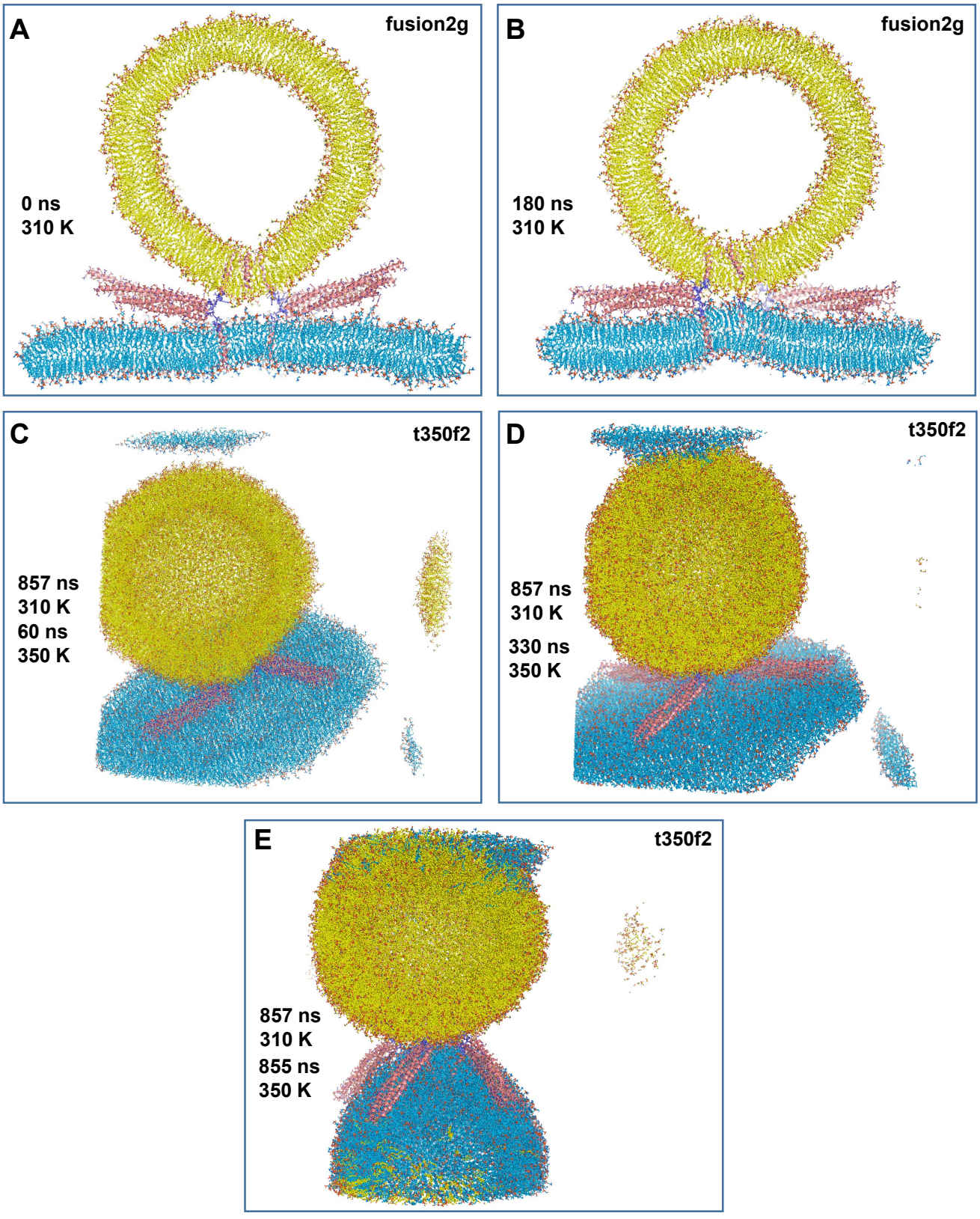
A
fusion2g
0 ns
310 K
B
fusion2g
180 ns
310 K
C
t350f2
857 ns
310 K
60 ns
350 K
D
t350f2
857 ns
310 K
330 ns
350 K
E
t350f2
857 ns
310 K
855 ns
350 K

Figure S2. MD simulation of four almost completely helical trans-SNARE complexes bridging a vesicle and a flat bilayer and close to the center of the interface. (*A*-*B*) Slices of the system in its initial configuration (*A*) and after 180 ns (*B*) of simulation at 310 K. The system of (*B*) was superimposed with the initial configuration to facilitate comparisons. (*C*-*E*) Overall view of the system after 857 ns of simulation at 310 K and 60 ns (*C*), 330 ns (*D*) and 855 ns (*E*) at 350 K. The systems were not superimposed with the initial configuration so that the effects of random translation and rotation can be observed. The parts of the system that moved out of the box used for periodic boundary conditions emerge at the opposite side of the box. The emergence of the edge of the flat bilayer at the top of the box led first to contact with the vesicle (*C*) and later to merger of the two bilayers (*D, E*). Lipids and proteins are shown as stick models, and SNARE complexes are in addition represented by ribbon diagrams. The color code is the same as in Fig. 1.

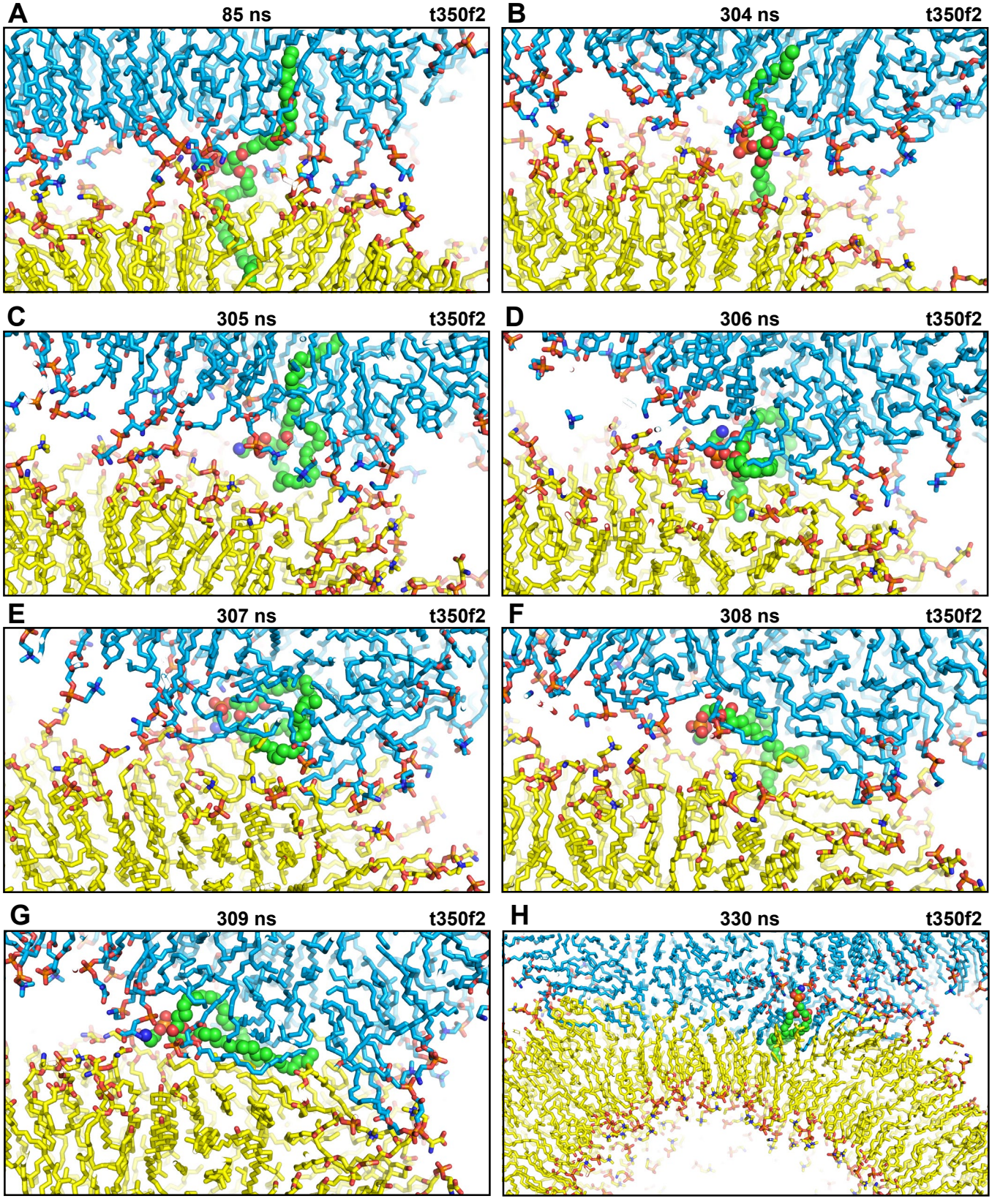
A
85 ns
t350f2
B
304 ns
t350f2
C
305 ns
t350f2
D
306 ns
t350f2
E
307 ns
t350f2
F
308 ns
t350f2
G
309 ns
t350f2
H
330 ns
t350f2

Figure S3. Snapshots taken at the indicated time points of the t350f2 simulation showing the splaying of an SDPE molecule at the interface between the edge of the flat bilayer and the vesicle, and the merger of the bilayers. Note that the SDPE molecule remained splayed for over 200 ns without the membrane merging. Membrane merger occurred when fluctuations of the SDPE molecule led to hydrophobic encounters at the polar interface. Lipids and proteins are shown as stick models, and SNARE complexes are in addition represented by ribbon diagrams. The color code is the same as in Fig. 1. The SDPE molecule is represented by spheres with nitrogen atoms in dark blue, oxygens in red, phosphorus in orange and carbons in green.

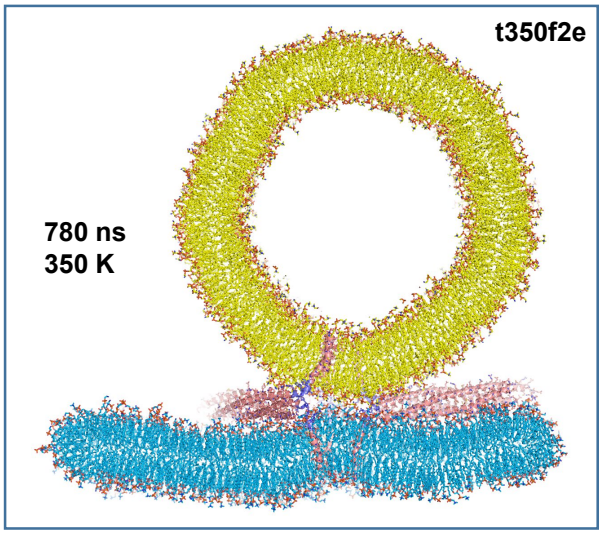

Figure S4. Slice showing the t350f2e system after 780 ns of simulation at 350 K. Lipids and proteins are shown as stick models, and SNARE complexes are in addition represented by ribbon diagrams. The color code is the same as in Fig. 1.

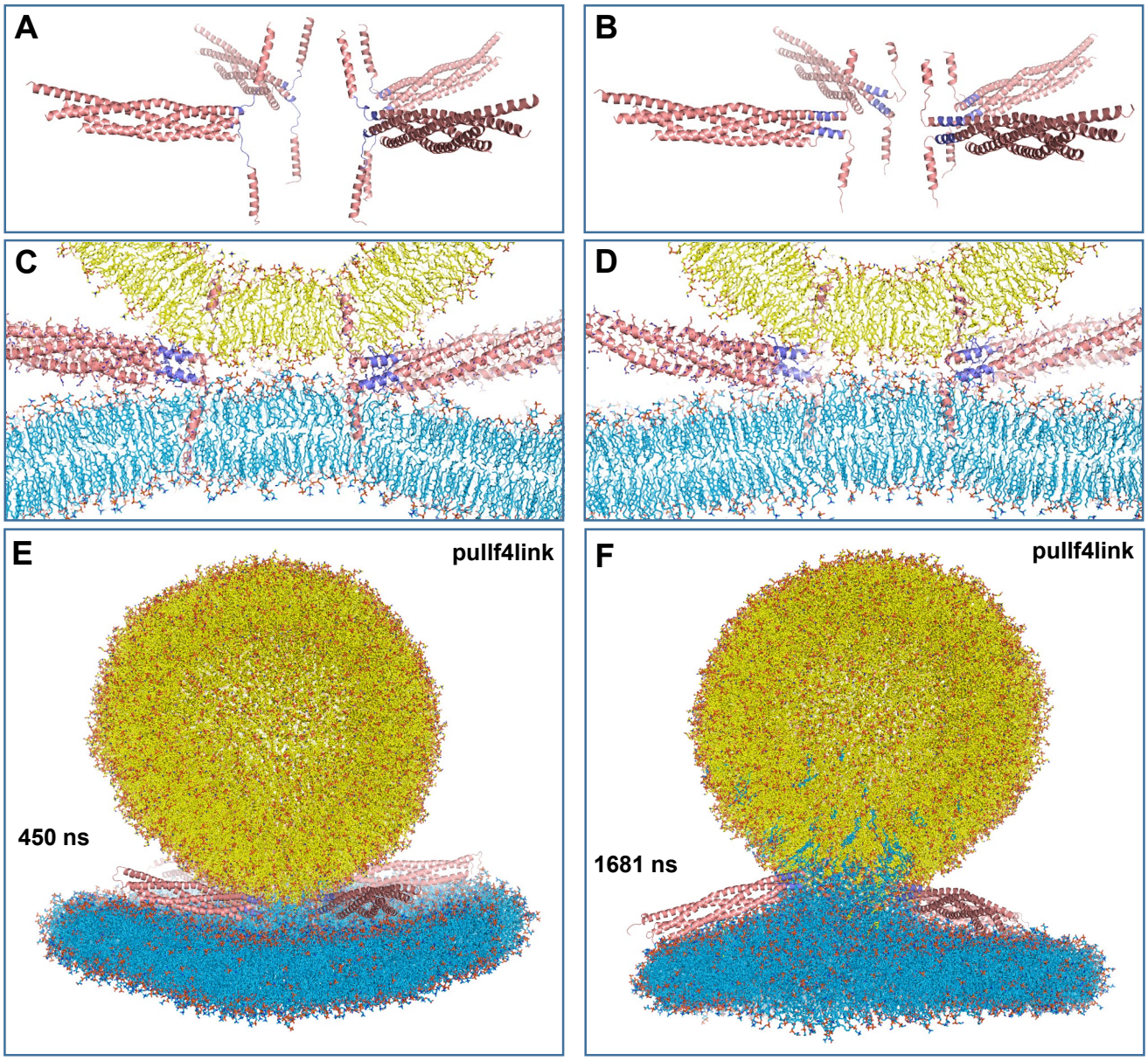

Figure S5. MD simulation of four trans-SNARE complexes bridging a vesicle and a flat bilayer, with the linkers zippered and a pulling force to keep them zippered. (*A*-*B*) Ribbon diagrams showing the initial configuration of the trans-SNARE complexes before using restrained MD simulations to zipper the linkers (*A*) and at the end of these simulations, with the linkers fully zippered (*B*). (*C*-*D*) Slices of the system showing the trans-SNARE complexes inserted into the flat bilayer and the vesicle in the initial configuration used for the pullf4link simulation, shown from opposite angles to display the four complexes. (*E*-*F*) Full views of the system at the indicated time points of the pullf4link simulation. Lipids and proteins are shown as stick models, and SNARE complexes are in addition represented by ribbon diagrams. The color code is the same as in Fig. 1.

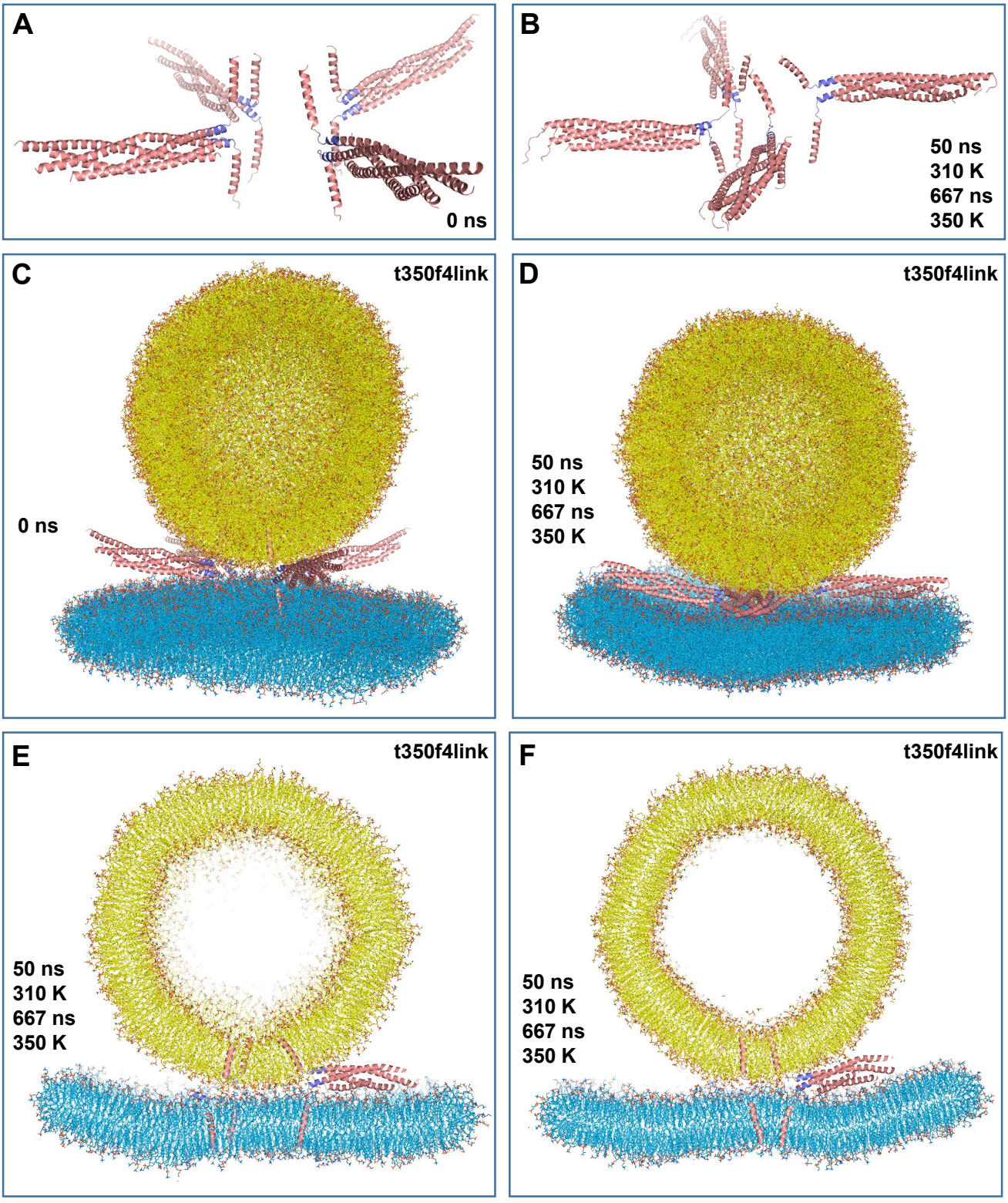
A
0 ns
B
50 ns
310 K
667 ns
350 K
C
t350f4link
0 ns
D
t350f4link
50 ns
310 K
667 ns
350 K
E
t350f4link
50 ns
310 K
667 ns
350 K
F
t350f4link
50 ns
310 K
667 ns
350 K

Figure S6. MD simulation of four trans-SNARE complexes bridging a vesicle and a flat bilayer, with the linkers zippered but no pulling force to keep them zippered (t350f4link simulation). (*A*) Ribbon diagram showing the initial configuration of the trans-SNARE complexes used for this simulation, which resulted from restrained MD simulations to zipper the linkers starting with the complexes shown in Fig. S5A. (*B*) Ribbon diagram of the trans-SNARE complexes at the end of the simulation. (*C-D*) Full views of the system at the indicated time points of the t350f4link simulation. (*E-F*) Slices of the system at the end of the simulation taken from different angles to show how the flat bilayer was somewhat buckled in one direction but not another. In (*C-F*), Lipids and proteins are shown as stick models, and SNARE complexes are in addition represented by ribbon diagrams. The color code is the same as in Fig. 1.

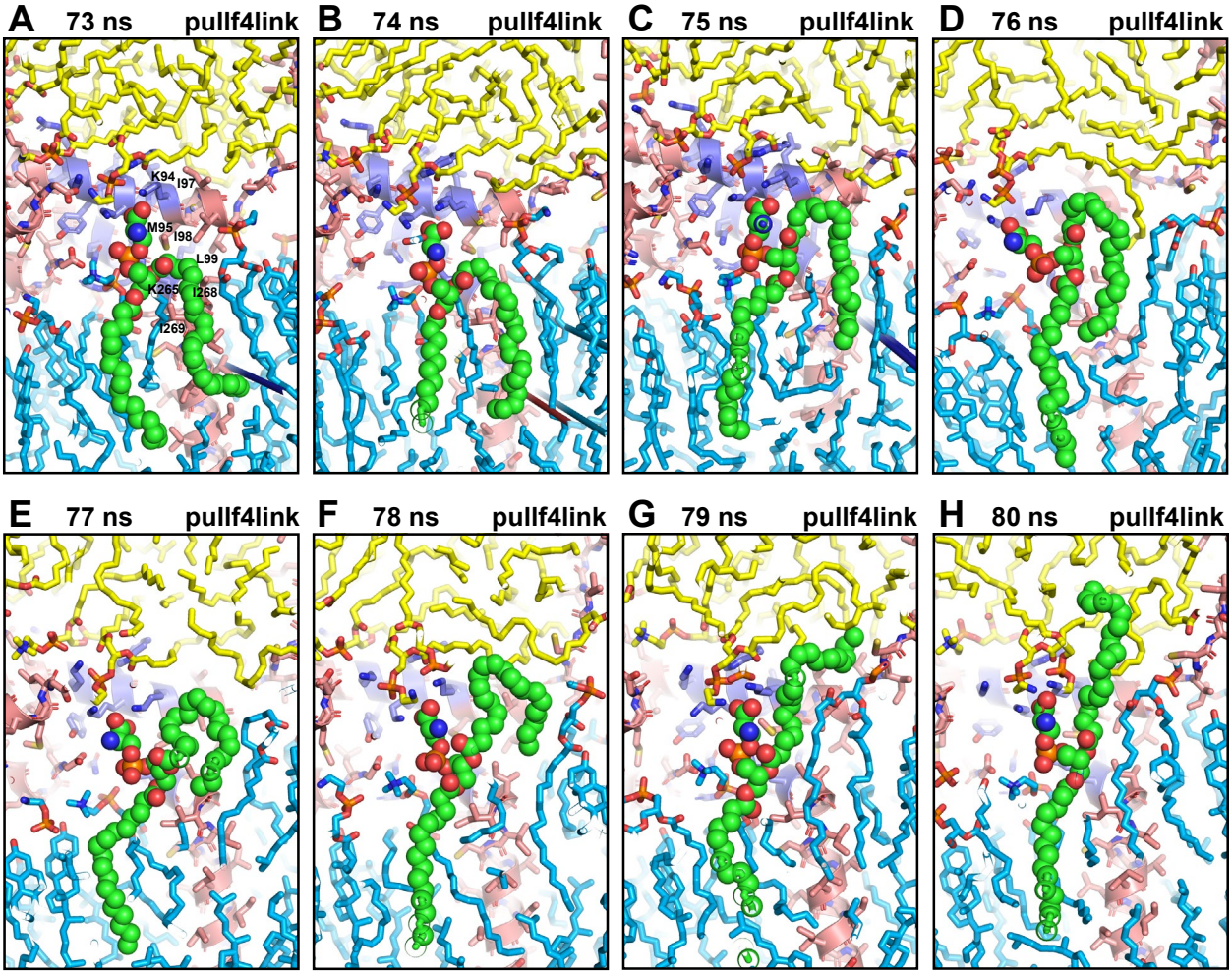

Figure S7. Snapshots taken at the indicated time points of the pullf4link simulation showing the splaying of an SDPS molecule catalyzed by the jxt linkers and TM regions of one of the trans-SNARE complexes. Lipids and proteins are shown as stick models, and SNARE complexes are in addition represented by ribbon diagrams. The color code is the same as in Fig. 1. The SDPS molecule is represented by spheres with nitrogen atoms in dark blue, oxygens in red, phosphorus in orange and carbons in green.

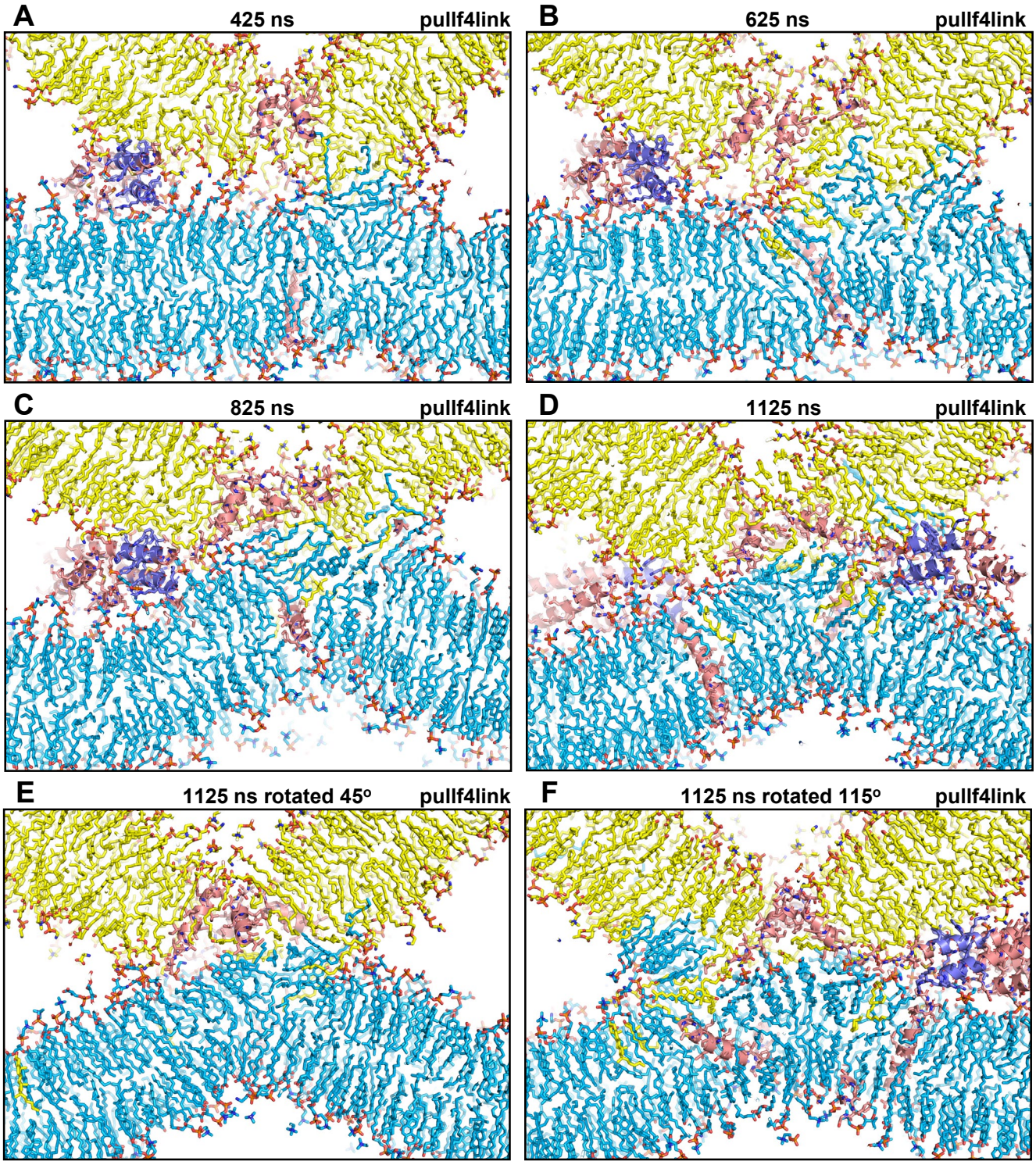

Figure S8. Snapshots of the pullf4link simulation showing the expansion of the hydrophobic nucleus into stalk-like structures. Panels (*A-D*) were taken at the indicated time points. Panels (*E,F*) show the same frame as (*D*) (at 1125 ns) but from different angles to illustrate the asymmetry of the lipid configuration at the interface, with some areas being purely hydrophobic whereas other areas contain lipid head groups that are normally close to the backbone of unstructured residues of the TM regions. Lipids and proteins are shown as stick models, and SNARE complexes are in addition represented by ribbon diagrams. The color code is the same as in Fig. 1.

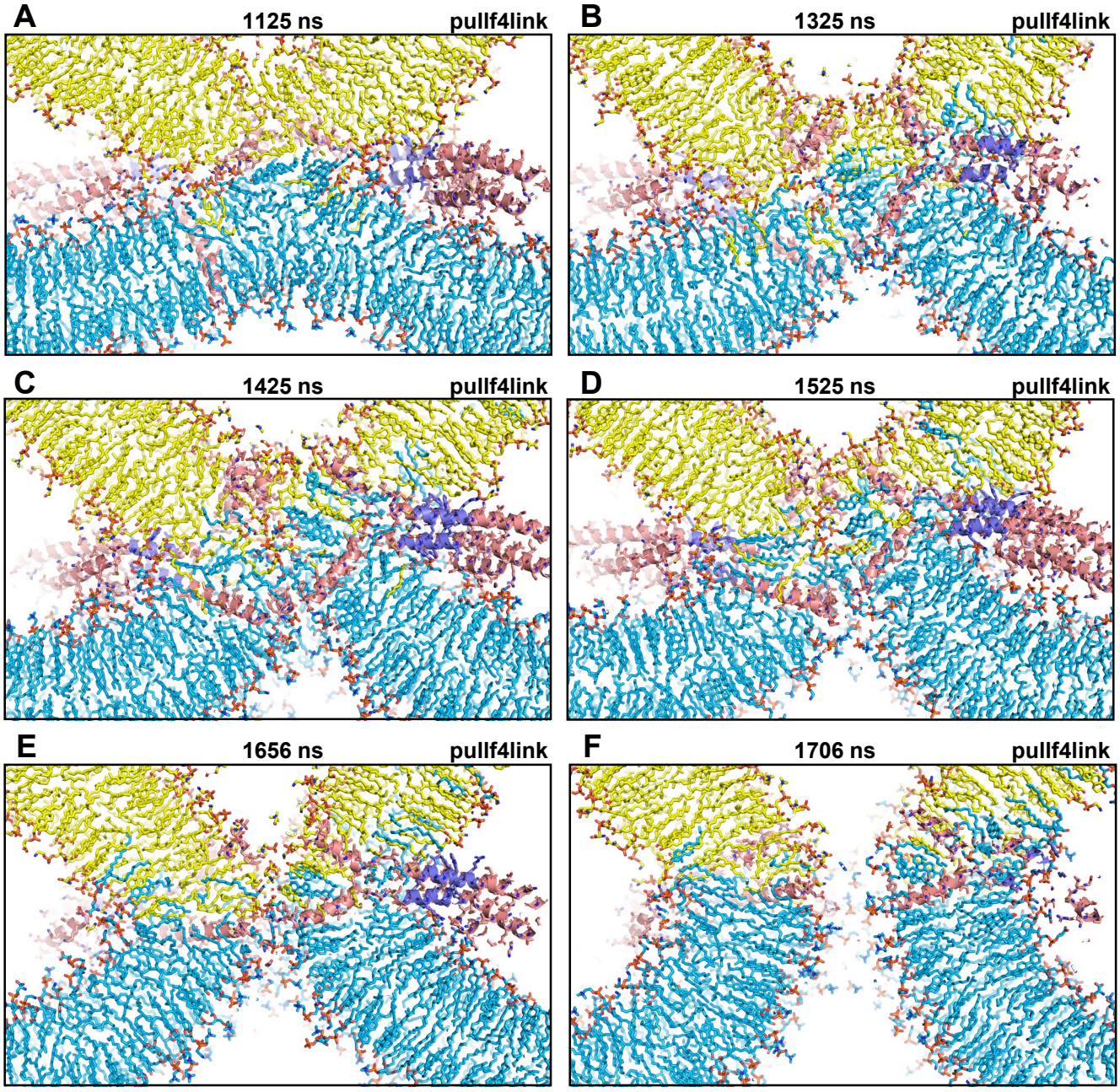

Figure S9. Snapshots taken at the indicated time points of the pullf4link simulation showing the evolution from stalk-like structures to the fusion pore. The diagrams show how the lipids were often quite disordered at the interface of the stalk-like structures and they became more ordered as they adopted the orientations that correspond to their positions in the developing fusion pore, most likely guided at least in part by the SNARE TM regions. Lipids and proteins are shown as stick models, and SNARE complexes are in addition represented by ribbon diagrams. The color code is the same as in Fig. 1.

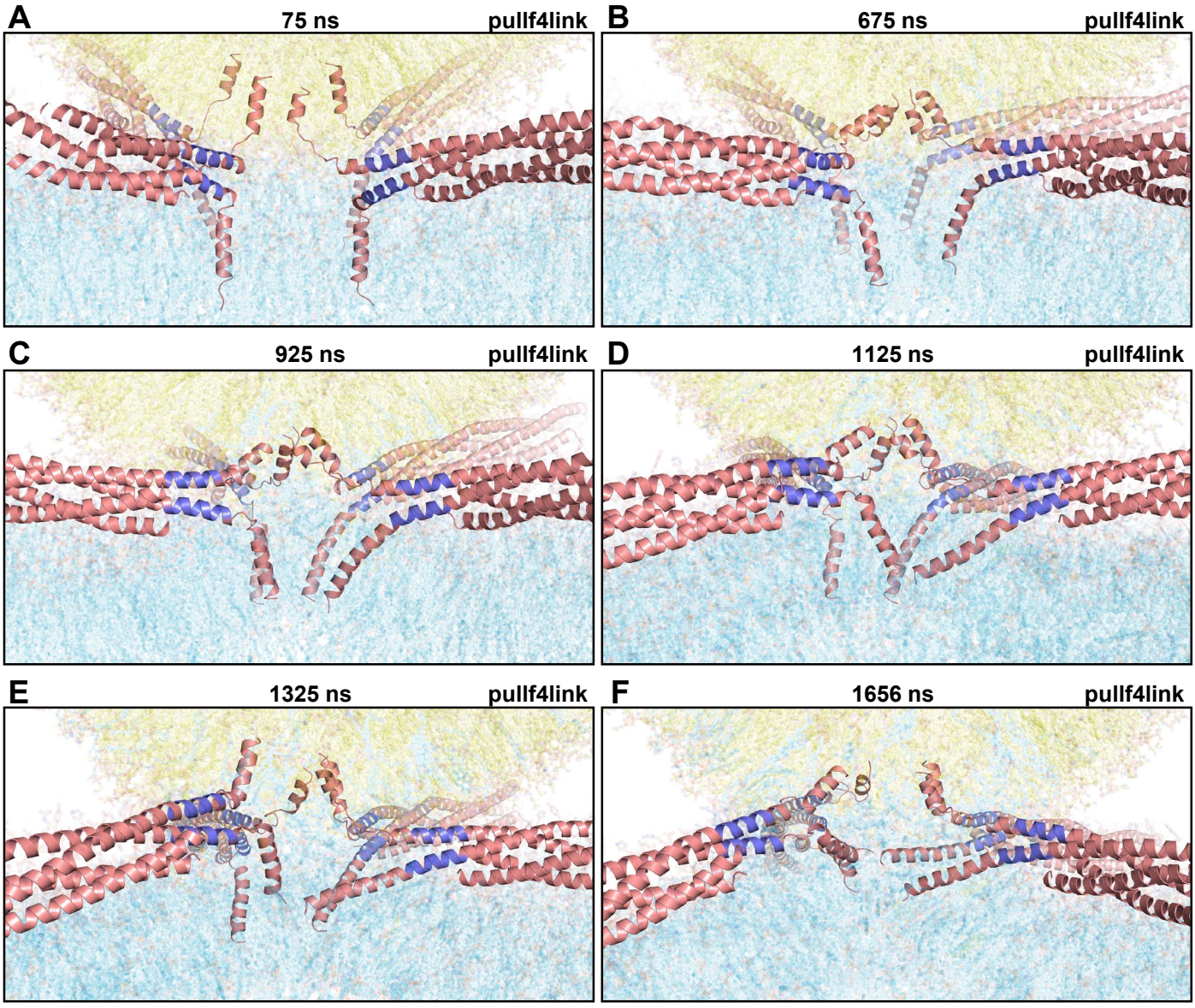

Figure S10. Snapshots taken at the indicated time points of the pullf4link simulation illustrating the conformational changes in the SNAREs as the system evolved from bilayer-bilayer contact to the fusion pore. SNARE complexes are represented by ribbon diagrams and lipids are represented by 90% transparent sticks to allow visualization of the ribbons. Note that the thickness of the slices shown in these panels is much larger than those of the slices shown in Figures 3, 4, S8, S9 so that all four trans-SNARE complexes can be observed, but the lipids then need to be transparent to allow visualization of the SNAREs. Panels (*A, C, E*) are those shown in Fig. 5, while panels (*B, D, F*) show additional time frames so that the evolution of TM conformations with time can be better appreciated. The color code is the same as in Fig. 1.

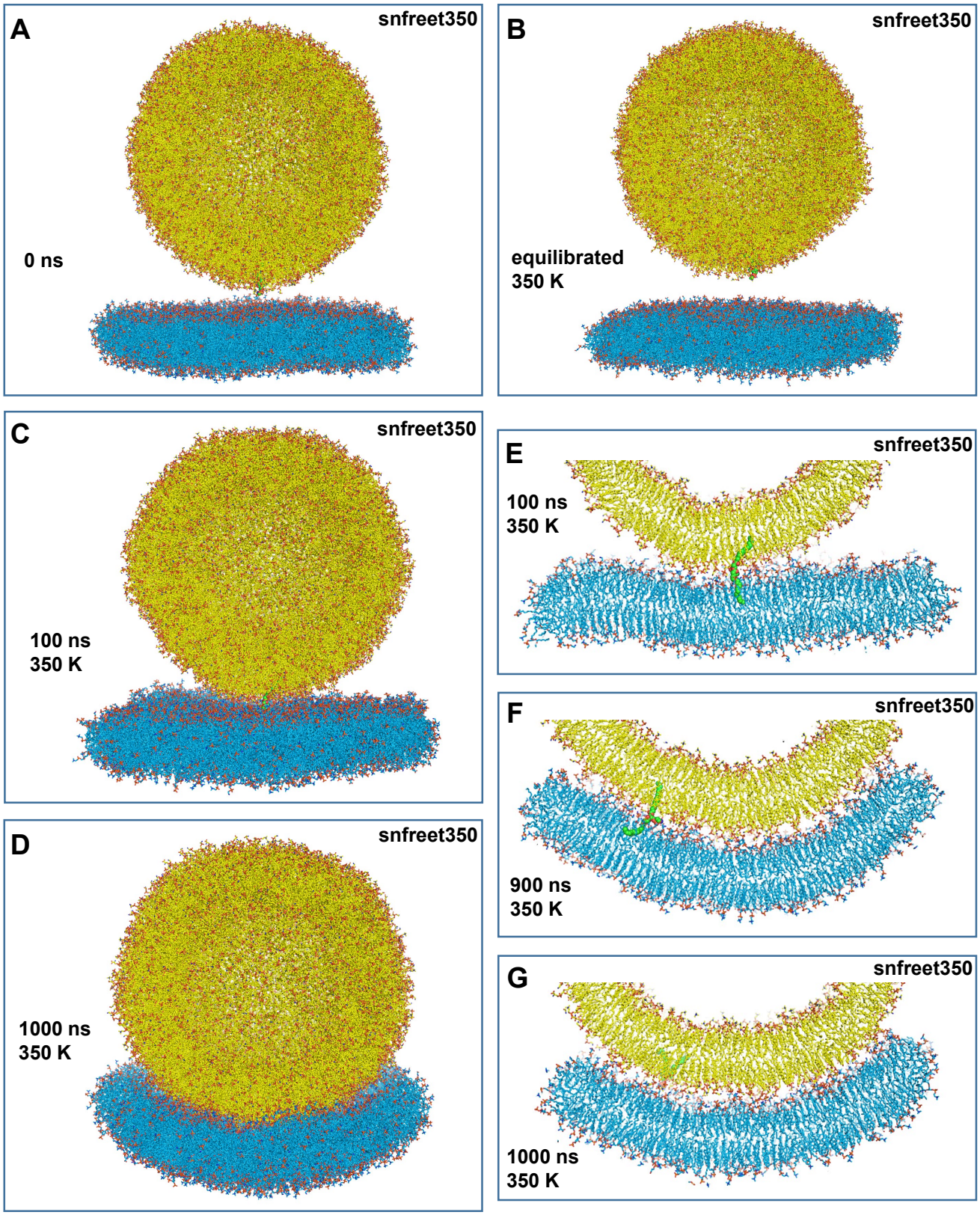
A
snfreet350
0 ns
B
snfreet350
equilibrated
350 K
C
snfreet350
100 ns
350 K
D
snfreet350
1000 ns
350 K
E
snfreet350
100 ns
350 K
F
snfreet350
900 ns
350 K
G
snfreet350
1000 ns
350 K

Figure S11. Simulation of a flat bilayer and a vesicle bridged by a splayed lipid. (*A*-*D*) Full views of the initial system (*A*), the system after temperature equilibration for 1 ns and pressure equilibration for 1 ns (*B*), and after 100 ns (*C*) or 1000 ns (*D*) of production simulation at 350 K. (*E*-*F*) Slices of the system taken at the indicated time points. Lipids and proteins are shown as stick models, and SNARE complexes are in addition represented by ribbon diagrams. The color code is the same as in Fig. 1. The splayed lipid is represented by spheres with nitrogen atoms in dark blue, oxygens in red, phosphorus in orange and carbon in green.

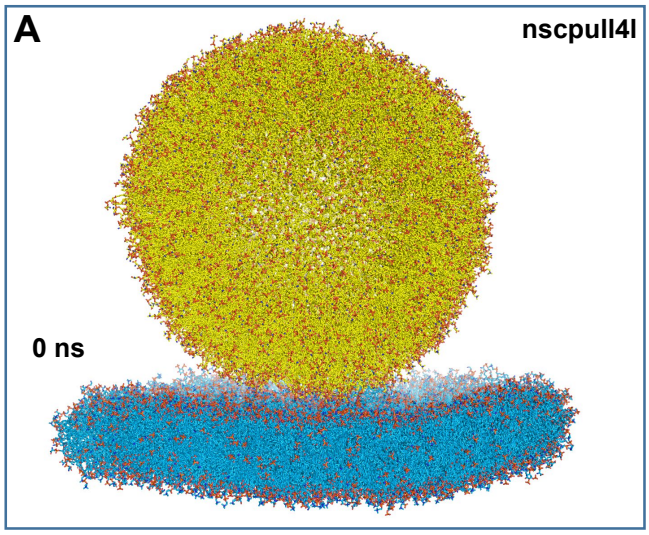
A
nscpull4l
0 ns

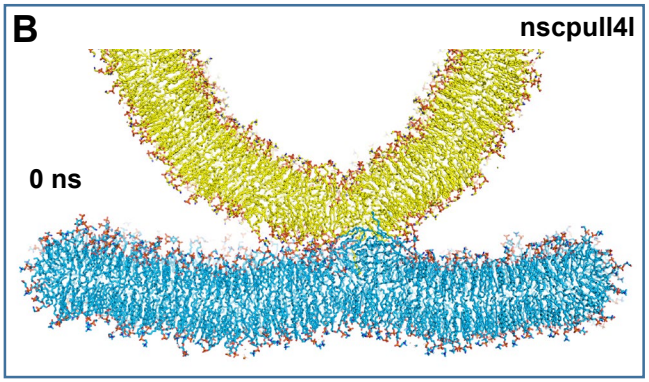
B
nscpull4l
0 ns

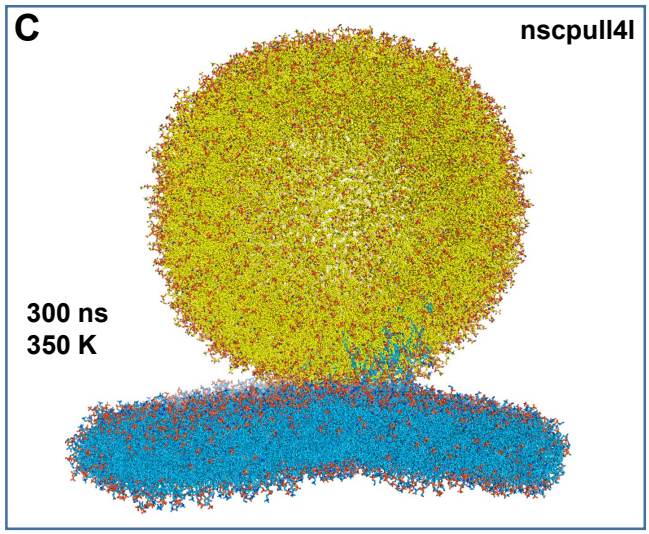
C
nscpull4l
300 ns
350 K

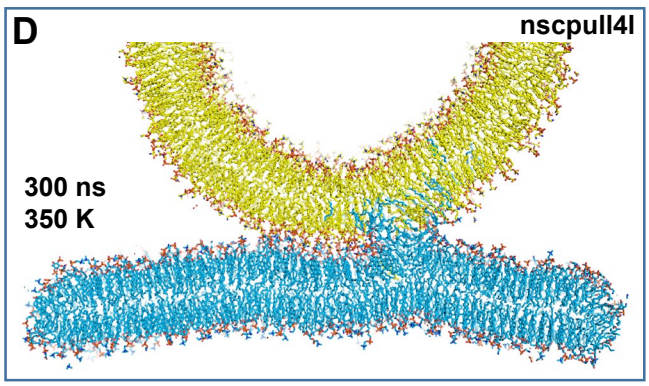
D
nscpull4l
300 ns
350 K

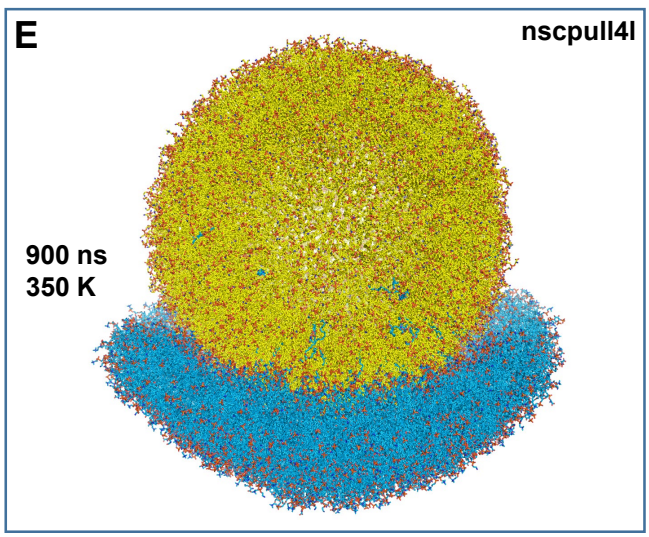
E
nscpull4l
900 ns
350 K

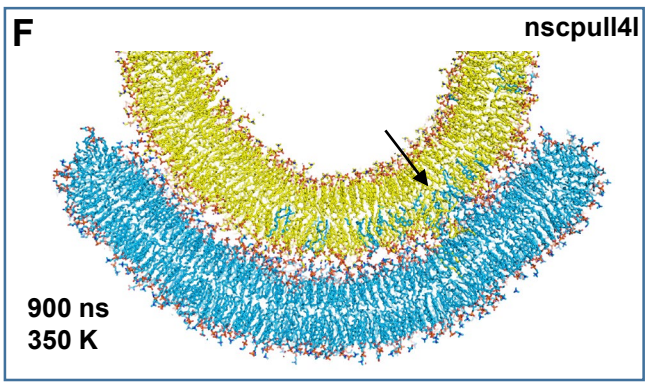
F
nscpull4l
900 ns
350 K

Figure S12. Simulation of a flat bilayer bridged to a vesicle by a few lipids that form a small hydrophobic core at the interface. (*A*) Initial configuration of the system, which was generated from the 475 ns frame of the pullf4link simulation by removing the SNAREs and replacing their TM regions with lipids. (*C,E*) Full view of the system after 300 ns (*C*) and 900 ns (*E*) of production simulation at 350 K. (*B,D,F*) Slices of the system at the stages shown in panels (*A,C,E*), respectively. The slice at 900 ns shows how the entire flat bilayer wraps around the vesicle and some of its lipids have been transferred to the vesicle. The arrow of panel (*F*) points at the hydrophobic core remaining at the polar interface.

Movie S1 (separate file). Movie showing slices of the pullf4link simulation from 0 to 1956 ns, illustrating the events that lead to membrane fusion.

SI References

1. H. J. Risselada, C. Kutzner, H. Grubmuller, Caught in the act: visualization of SNARE-mediated fusion events in molecular detail. *Chembiochem* **12**, 1049-1055 (2011).
2. V. Knecht, S. J. Marrink, Molecular dynamics simulations of lipid vesicle fusion in atomic detail. *Biophys J* **92**, 4254-4261 (2007).
3. X. Zhuang, J. R. Makover, W. Im, J. B. Klauda, A systematic molecular dynamics simulation study of temperature dependent bilayer structural properties. *Biochim Biophys Acta* **1838**, 2520-2529 (2014).
4. D. Fasshauer, D. Bruns, B. Shen, R. Jahn, A. T. Brunger, A structural change occurs upon binding of syntaxin to SNAP-25. *J. Biol. Chem* **272**, 4582-4590 (1997).
5. J. Hazzard, T. C. Sudhof, J. Rizo, NMR analysis of the structure of synaptobrevin and of its interaction with syntaxin. *J. Biomol. NMR* **14**, 203-207 (1999).
6. I. Dulubova *et al.*, A conformational switch in syntaxin during exocytosis: role of munc18. *EMBO J* **18**, 4372-4382 (1999).
7. R. W. Baker *et al.*, A direct role for the Sec1/Munc18-family protein Vps33 as a template for SNARE assembly. *Science* **349**, 1111-1114 (2015).
8. K. P. Stepien, J. Xu, X. Zhang, X. C. Bai, J. Rizo, SNARE assembly enlightened by cryo-EM structures of a synaptobrevin-Munc18-1-syntaxin-1 complex. *Sci Adv* **8**, eabo5272 (2022).
9. C. S. Kim, D. H. Kweon, Y. K. Shin, Membrane topologies of neuronal SNARE folding intermediates. *Biochemistry* **41**, 10928-10933 (2002).
10. J. Rizo, L. Sari, Y. Qi, W. Im, M. M. Lin, All-atom molecular dynamics simulations of Synaptotagmin-SNARE-complexin complexes bridging a vesicle and a flat lipid bilayer. *Elife* **11**, e76356 (2022).
11. Y. Hu, L. Zhu, C. Ma, Structural Roles for the Juxtamembrane Linker Region and Transmembrane Region of Synaptobrevin 2 in Membrane Fusion. *Front Cell Dev Biol* **8**, 609708 (2020).
12. J. Kesavan, M. Borisovska, D. Bruns, v-SNARE actions during Ca(2+)-triggered exocytosis. *Cell* **131**, 351-363 (2007).
13. M. Dhara *et al.*, v-SNARE transmembrane domains function as catalysts for vesicle fusion. *Elife* **5** (2016).
14. B. Hastoy *et al.*, A Central Small Amino Acid in the VAMP2 Transmembrane Domain Regulates the Fusion Pore in Exocytosis. *Sci Rep* **7**, 2835 (2017).
15. G. Vardar, A. Salazar-Lazaro, S. Zobel, T. Trimbuch, C. Rosenmund, Syntaxin-1A modulates vesicle fusion in mammalian neurons via juxtamembrane domain dependent palmitoylation of its transmembrane domain. *Elife* **11**, e78182 (2022).
16. P. Zhou, T. Bacaj, X. Yang, Z. P. Pang, T. C. Sudhof, Lipid-anchored SNAREs lacking transmembrane regions fully support membrane fusion during neurotransmitter release. *Neuron* **80**, 470-483 (2013).
17. A. Stein, G. Weber, M. C. Wahl, R. Jahn, Helical extension of the neuronal SNARE complex into the membrane. Nature 460, 525-528 (2009).